Food Microbiology 140 (2026) 105151

Contents lists available at ScienceDirect

Food Microbiology

journal homepage: www.elsevier.com/locate/fm

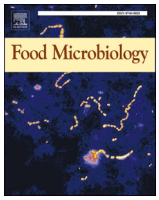

Microbial succession and spoilage dynamics revealed by multi-omics in Norway lobster (*Nephrops norvegicus*) during ice storage

Ahmed Elsheshtawy [a,b,*], Benjamin G.J. Clokie [a], Sasha Saugh [a,f], Karen D. Adler [c], Slawomir M. Michniewski [c], Simon MacKenzie [a], Martha R.J. Clokie [c], Thomas Sicheritz-Pontén [d,e], Amaya Albalat [a]

[a] Institute of Aquaculture, University of Stirling, Stirling, FK9 4LA, United Kingdom
[b] Faculty of Aquatic and Fisheries Sciences, Kafrelsheikh University, Kafr El Sheikh City, 33516, Egypt
[c] Becky Mayer Centre for Phage Research, Division of Microbiology and Infection, University of Leicester, Leicester, LE1 7RH, United Kingdom
[d] Center for Evolutionary Hologenomics, Globe Institute, University of Copenhagen, Copenhagen, Denmark
[e] Centre of Excellence for Omics-Driven Computational Biodiscovery (COMBio), Faculty of Applied Sciences, AIMST University, Bedong, Malaysia
[f] Aquaglobal Veterinary Consulting Pty Ltd., Durban, 4037, South Africa

ARTICLE INFO

Keywords:
Seafood spoilage
Amplicon sequencing
Metagenomics
Crustaceans
Shelf-life
Moritella

ABSTRACT

The Norway lobster (*Nephrops norvegicus*) is a high-value seafood product with limited shelf-life under chilled storage. This study investigated microbial succession and spoilage dynamics during ice storage (0 °C, 16 days) using an integrated multi-omics approach combining sensory assessment (Quality Index Method), physicochemical indicators (muscle pH and K-value), culture-dependent microbiology, absolute bacterial load quantification (16S rRNA qPCR), 16S rRNA gene amplicon sequencing and shotgun metagenomics.

Quality deterioration was characterised by progressive increases in sensory scores, nucleotide degradation and muscle pH, with rejection occurring at day 7. This transition coincided with a marked increase in bacterial load following an initial lag phase (days 0-5), indicating a critical shift in spoilage progression. Amplicon sequencing revealed a transition from a diverse early community (days 0-3) to a *Proteobacteria*-dominated assemblage from day 5 onwards, driven by increases in *Moritella*, *Pseudoalteromonas* and *Aliivibrio*. Metagenomic analysis further resolved these dynamics at species-level resolution and identified a limited number of dominant taxa associated with mid-to late-stage spoilage.

The convergence of sensory rejection, physicochemical changes and microbial restructuring identifies a mid-storage tipping point in spoilage development. By integrating multi-omics with established quality indicators, this study links microbial succession to measurable spoilage outcomes. The dominant taxa are consistent with known spoilage-associated activities, including proteolysis and off-odour production, while highlighting *Moritella* as a potential contributor in crustacean spoilage. These findings provide a temporal framework for spoilage progression in *N. norvegicus* and inform targeted strategies for shelf-life management.

1. Introduction

Advances in high-throughput sequencing have transformed our understanding of food spoilage microbiology by enabling culture-independent profiling of entire microbial communities within complex food ecosystems. The application of these technologies has marked the emergence of the 'FoodOmics' era (Anagnostopoulos et al., 2022). Among these approaches, amplicon-based 16S rRNA gene sequencing has become a cost-effective, high-throughput tool for in-depth characterisation of microbial dynamics in seafood spoilage studies (Odeyemi et al., 2019; Parlapani et al., 2020). Moreover, shotgun whole-genome metagenomics provides higher taxonomic resolution and enables exploration of the functional potential of spoilage-associated taxa (Sequino et al., 2024). Integrating multiple omics tools facilitates a more holistic understanding of spoilage processes by enabling the identification of microbial interactions and functional genes potentially responsible for organoleptic deterioration (Cocolin et al., 2018). Consequently, recent research has emphasised the importance of

* Corresponding author. Institute of Aquaculture, University of Stirling, Pathfoot Building, Stirling, FK9 4LA, United Kingdom.
E-mail address: a.m.ahmed@stir.ac.uk (A. Elsheshtawy).

https://doi.org/10.1016/j.fm.2026.105151
Received 31 March 2026; Received in revised form 11 May 2026; Accepted 12 May 2026
Available online 13 May 2026
0740-0020/© 2026 The Authors. Published by Elsevier Ltd. This is an open access article under the CC BY license (http://creativecommons.org/licenses/by/4.0/).

longitudinal, integrative approaches that link sensory quality, biochemical freshness indices and microbial community dynamics over time.

Such approaches are particularly relevant for seafood products given their inherent perishability. As recently reviewed by Wang and Zheng (2025), seafood products are prone to rapid spoilage due to high moisture content that favours bacterial proliferation, low connective tissue levels that render proteins susceptible to enzymatic degradation, elevated levels of free amino acids and non-protein nitrogenous compounds and a low to neutral muscle pH. Furthermore, seafood products are shipped internationally, and many serve high-value markets. This is the case for Norway lobster (*Nephrops norvegicus),* also marketed as langoustine, scampi or Dublin Bay prawn, which represents one of the most valuable fisheries in the UK (annual value > £100 million) and across Europe (MMO, 2025). Although it holds high commercial value and strong consumer preference for whole fresh products in international markets, *N. norvegicus* is highly perishable (Gornik et al., 2013). This short shelf-life imposes significant logistical and economic constraints across the supply chain and contributes substantially to product losses.

Post-harvest spoilage of *N. norvegicus* is driven by a combination of biochemical reactions (e.g. enzymatic activity and oxidation) and microbial activity. Following death, autolytic enzymes catalyse the degradation of adenosine triphosphate (ATP) into lower nucleotide catabolites, resulting in progressive losses in flavour, odour and texture that are reflected in biochemical freshness indices such as the K-value (Albalat et al., 2011). Concurrently, melanosis develops through the action of polyphenol oxidase on tyrosine and related phenolic substrates, leading to the formation of melanin and visible blackening of the carapace (Coates and Albalat, 2014; Rolle et al., 1991). Although melanosis is primarily an aesthetic defect, it markedly accelerates consumer rejection and reduces marketability. Thus, several liquid-based antimelanotic treatments have been developed to preserve visual quality (Martı'nez-Alvarez et al., 2007). While these treatments can effectively delay colour changes, they do not prevent microbial spoilage, which ultimately determines sensory shelf life under iced storage.

Microbial spoilage is the dominant cause of quality loss in chilled seafood products. The nutrient-rich composition, high water activity and pH of crustacean muscle provide ideal conditions for bacterial growth. Spoilage is typically driven by specific spoilage organisms (SSOs) that are selectively favoured by cold storage conditions and whose metabolic activity generates volatile compounds responsible for off-odours, slime formation and flavour defects (Gram and Dalgaard, 2002). In *N. norvegicus*, culture-based studies have implicated psychrotolerant marine *Gammaproteobacteria* such as *Photobacterium*, *Pseudoalteromonas, Pseudomonas* and *Psychrobacter* as key spoilage organisms (Boziaris et al., 2011; Gornik et al., 2011). However, these approaches capture only the culturable fraction of the microbiome and may underestimate the complexity and succession of spoilage communities (Cao et al., 2017). In addition, previous studies have largely relied on single-method approaches or have not integrated microbial community dynamics with quantitative spoilage indicators over time, limiting the ability to define biologically meaningful transition points in spoilage progression. Therefore, an in-depth understanding of critical spoilage transitions and the taxa dominating each phase is essential for the rational development of targeted preservation strategies, including emerging biological interventions such as bacteriophages (Artawinata et al., 2023).

In this study, we applied an integrated experimental framework to characterise spoilage development in *N. norvegicus* during ice storage. By combining sensory assessment, physicochemical indicators, culture-dependent microbiology, absolute bacterial load quantification, 16S rRNA gene amplicon sequencing and shotgun metagenomics, we aimed to resolve microbial succession across multiple biological scales. Specifically, we sought to identify critical transition points in spoilage progression and define the dominant taxa associated with this shift at species-level resolution. This approach provides an integrated temporal framework linking microbial dynamics with measurable spoilage outcomes in a high-value crustacean system.

2. Materials and methods

2.1. Ethics statement

This study was conducted in accordance with the United Kingdom Animals (Scientific Procedures) Act. All experimental procedures were approved by the University of Stirling Animal Welfare and Ethical Review Body (AWERB approval number: 2022 7912 6319).

2.2. Experimental design and sampling protocol

A time-controlled ice storage experiment was conducted to investigate bacterial spoilage dynamics in *N. norvegicus*. A total of 120 lobsters were captured by a commercial otter trawl in the Clyde Sea area, Scotland, UK (55°36′39.0″ N, 4°52′59.4″ W; depth 60-80 m). Trawling was carried out using the commercial vessel *Eilidh Anne*, equipped with a single hopper trawl net with a nominal cod-end mesh size of 80 mm, towed at approximately 2 knots for ~2 h. Animals were brought on board at approximately 17:00.

Following capture, animals were washed with running seawater and stored in crates without water or ice, in accordance with standard commercial practice, with an estimated catch-to-landing time of ~1 h. No anti-melanotic treatments were applied. Upon landing, animals were packed individually in polyethylene bags and stored on ice in insulated polystyrene boxes. Boxes were transported to the University of Stirling, Scotland, UK within 2 h and maintained in a temperature-controlled cold room at 4 °C for up to 16 days. Ice levels were checked daily and replenished every second day. All boxes were handled and packed identically to minimise variability in storage conditions. This controlled storage design minimised handling variability and enabled the first high-resolution characterisation of spoilage-associated microbial succession in *Nephrops norvegicus* under ice-storage conditions.

On visual inspection, animals appeared healthy with no obvious lesions or abnormalities. Mean carapace length was 37.7 ± 3.6 mm, with a sex ratio of 32% males and 68% females; 42% of individuals were soft-shelled and 58% hard-shelled.

Animals were sampled immediately after removal from cold storage on days 0, 1, 3, 5, 7, 10, 13 and 16. At the first two sampling points (days 0 and 1), animal responsiveness was assessed by mechanical stimulation of the mouthparts prior to sampling, and animals were subsequently killed by splitting, involving destruction of the main ganglia, prior to further processing. At each time point, 14 individuals were randomly selected. From these, seven animals were randomly assigned to each of two complementary sampling protocols (sampling protocols A and B), designed to allow parallel microbiological, molecular, physicochemical and sensory analyses.

Sampling protocol A focused on culture-dependent and DNA-based microbiological analyses. Tail muscle (abdominal flexor muscle) was sampled aseptically. Samples were used for determination of total viable counts (TVC) using plate-based methods (n = 3 per time point), bacterial 16S rRNA gene quantification by qPCR (n = 7 per time point), 16S rRNA gene amplicon sequencing and whole-genome shotgun metagenomic sequencing. Samples for molecular analyses were preserved in DNA/RNA Shield (Zymo Research, USA) and stored at −20 °C until processing.

Sampling protocol B focused on quality assessment and physicochemical measurements. Whole-animal sensory evaluation was performed using the Quality Index Method (QIM), except at day 0. Following sensory assessment, tail muscle samples were collected for the determination of muscle pH and nucleotide degradation products, expressed as K-values.

2.3. Sensory assessment

Sensory quality of raw *N. norvegicus* (n = 7 per sampling day) was evaluated using the Quality Index Method (QIM), following the scheme developed by Gornik et al. (2013). The assessment was based on changes in odour and appearance of the dorsal and ventral aspects of the claws, the dorsal aspect of the cephalothorax (including the eyes), and the dorsal and ventral tail. Five sensory attributes were scored using a four-point demerit scale (0-3), with increasing scores indicating progressive loss of freshness. Prior to assessment, samples were equilibrated to room temperature. Sensory evaluation was performed at each sampling time point except day 0.

2.4. Physicochemical analyses of tail muscle

2.4.1. Muscle pH

Muscle pH was measured using abdominal flexor muscle samples (n = 7 per sampling day). Approximately 1 g of tissue per sample was homogenised in distilled water at a ratio of 1:10 (w/v), following Chiou and Huang (2004). Homogenisation was performed using an Ultra-Turrax homogeniser (IKA-Werke, Germany), and pH was measured using a calibrated glass-bodied pH meter (Jenway, Model 3505, UK).

2.4.2. ATP and nucleotide degradation products (K-values)

Nucleotide extraction and analysis were performed on tail muscle samples (n = 7 per sampling day) to assess freshness using K-values. Nucleotide extracts were prepared as described by Ryder (1985) and analysed as described in Albalat et al. (2009). Standard curves were prepared using adenosine 5′-triphosphate (ATP), adenosine 5′-diphosphate (ADP), adenosine 5′-monophosphate (AMP), inosine 5′-monophosphate (IMP), inosine (HxR) and hypoxanthine (Hx) standards (Sigma-Aldrich, UK). K-values were calculated according to Saito et al. (1959):

$$\text{K-value}\ (\%) = 100 \times \frac{(\text{HxR} + \text{Hx})}{(\text{ATP} + \text{ADP} + \text{AMP} + \text{IMP} + \text{HxR} + \text{Hx})}$$

2.5. Microbiological analysis of tail muscle

Total viable counts (TVC) were determined from tail muscle samples to quantify bacterial load during ice storage. Isolated tails (n = 3 per sampling day) were surface-sterilised, and a portion of abdominal flexor muscle (0.4-1.0 g) was aseptically transferred to sterile stomacher bags. Samples were homogenised in sterile saline solution water (SSW) containing 0.1% bacteriological peptone (Difco™, BD, USA) at a ratio of 1:10 (w/v) using a Seward Stomacher® (Biomaster 80, Seward Ltd., UK), with two homogenisation cycles of 2 min at high speed. Homogenates were serially diluted in SSW, and 100 μL aliquots were spread-plated in triplicate onto tryptic soy agar supplemented with 2% (w/v) NaCl (TSA + 2% NaCl; Oxoid, UK). Plates were incubated at 22 °C for 48 h, and bacterial counts were recorded as colony-forming units per gram of muscle (cfu g^{-1}). Colonies were enumerated using a Stuart™ colony counter (DWK Life Sciences, UK). Representative colonies were selected for identification using matrix-assisted laser desorption/ionisation time-of-flight mass spectrometry (MALDI-TOF MS). Selected isolates were further characterised by 16S rRNA gene Sanger sequencing to confirm taxonomic affiliation.

2.6. Molecular analysis of tail muscle

2.6.1. DNA extraction and quantification

DNA was extracted from tail muscle samples (n = 7 per sampling day) using the E.Z.N.A.® Tissue DNA Kit (Omega Bio-Tek Inc., USA), following the manufacturer's instructions with minor modifications. Samples were homogenised using a bead beater homogeniser (Mini-Beadbeater 24, USA). To enhance DNA recovery from Gram-positive bacteria, homogenised samples were incubated at 95 °C for 10 min prior to the lysis step, as described by Elsheshtawy et al. (2023). DNA was eluted from the HiBind® DNA mini columns using the elution buffer supplied with the kit. DNA purity and concentration were initially assessed using a NanoDrop ND-1000 spectrophotometer (Thermo Fisher Scientific, Gloucester, UK), and DNA concentrations were subsequently confirmed using a Qubit 2.0 fluorometer (Thermo Fisher Scientific, USA).

2.6.2. Bacterial 16S rRNA quantification

Bacterial load in the abdominal flexor muscle of *N. norvegicus* (n = 7 per sampling day) was quantified by absolute quantitative PCR (qPCR) targeting the bacterial 16S rRNA gene, following the method described by Clokie et al. (2022). The V3-V4 region of the 16S rRNA gene was amplified in the DNA samples using the forward primer 314F and the reverse primer 805R and a FAM-labelled minor groove binder (MGB) TaqMan probe (Supplementary Table S1). qPCR reactions were performed in triplicate using SensiFAST™ Probe Lo-ROX Mix (Bioline, UK) on an Mx3005P real-time qPCR system (Agilent Technologies, Stratagene, USA). Thermal cycling conditions consisted of an initial denaturation at 95 °C for 10 min, followed by 40 cycles of denaturation at 95 °C for 30 s and annealing/extension at 60 °C for 1 min.

2.6.3. Bacterial 16S rRNA gene amplicon sequencing

Bacterial community composition in tail muscle was characterised by 16S rRNA gene amplicon sequencing. Amplicon libraries were generated from muscle DNA samples (n = 6 per sampling day), a negative sequencing control (NSC), a no-template control (NTC) and IoA microbiome standard (a mixture of DNA extracted from five bacterial species known to colonise aquatic species: *Aeromonas hydrophila* NCIMB 9240, *Edwardsiella ictaluri* NCIMB 13272, *Pseudomonas aeruginosa* ATCC 27853, *Vibrio anguillarum* NCIMB 6, and *Yersinia ruckeri* NCIMB 2194), following the approach described by Elsheshtawy et al. (2021). Template DNA was normalised to an equal bacterial load (1×10^6 16S rRNA gene copy numbers per reaction) based on absolute qPCR quantification results, in order to generate comparable 16S rRNA gene amplicon libraries across samples. Illumina amplicon libraries were prepared using a two-step PCR protocol. In the first PCR, the V4 region of the bacterial 16S rRNA gene was amplified using primers containing Illumina overhang adaptor sequences (Supplementary Table S1). In the second PCR, unique dual-index barcodes were added to the 5′ and 3′ ends of each amplicon using the Nextera XT Index Kit (Illumina, USA). Following amplification, libraries were pooled in equimolar concentrations and sequenced on an Illumina MiSeq platform by the Genomic Pipelines Group at the Earlham Institute (Norwich, UK).

2.6.4. Shotgun metagenomic sequencing

Shotgun metagenomic sequencing was performed to obtain species-level resolution of spoilage-associated bacteria in *N. norvegicus* tail muscle during ice storage. Muscle DNA samples were selected from three storage time points representing early, intermediate and late stages of spoilage (days 0, 7 and 16). For each time point, six biological replicates were analysed (n = 6 per sampling day).

Muscle DNA was sent to Novogene (Cambridge, UK) for library preparation and sequencing. DNA quality and concentration were assessed prior to library construction to ensure suitability for metagenomic sequencing. Sequencing libraries were prepared according to Novogene's standard protocols and sequenced on an Illumina platform to generate paired-end reads.

2.7. Bioinformatics and statistical analysis

Amplicon sequencing data were analysed following the pipeline described by Elsheshtawy et al. (2021); Martin et al. (2025). Briefly, raw sequence data were processed using the Mothur software package

(Schloss Patrick et al., 2009). Sequences were quality-filtered and clustered into operational taxonomic units (OTUs) at 97% sequence identity. Taxonomic assignment and generation of shared community and genus-level abundance tables were performed using the SILVA reference database (Quast et al., 2013). All statistical analyses were performed in RStudio (version 1.2.5042). Data normality was assessed using the Shapiro-Wilk test prior to statistical testing. When data met the assumptions of normality, differences among groups were analysed using one-way analysis of variance (ANOVA), followed by pairwise comparisons using *t*-test. For data that were not normally distributed, differences were assessed using the Kruskal-Wallis test, with pairwise comparisons performed using the Wilcoxon rank-sum test. In all cases, *p*-values were adjusted for multiple testing using the Benjamini-Hochberg (BH) correction (Benjamini and Hochberg, 1995), and statistical significance was accepted at $p < 0.05$. Statistical analyses were conducted using the *rstatix* package, and figures were generated using the *ggplot2* and *ggpubr* packages (Kassambara, 2020; Wickham, 2016). Alpha-diversity indices were calculated using the *phyloseq* package (McMurdie and Holmes, 2013). Beta-diversity was assessed using Bray-Curtis dissimilarities calculated with the *vegan* and *phyloseq* packages and visualised by principal coordinates analysis (PCoA) (Oksanen et al., 2013). Differences in community composition among groups were tested using permutational multivariate analysis of variance (PERMANOVA) implemented in the *vegan* package with 1002 permutations. Comparisons of relative abundances of individual taxa between groups were performed using the Wilcoxon rank-sum test, followed by Benjamini-Hochberg false discovery rate (FDR) correction.

Metagenomic reads from lobster muscle samples were first quality controlled using AdapterRemoval for trimming and cleaning (Schubert et al., 2016), followed by FastQC for quality assessment. Reads were then mapped to the available lobster reference genome (*Homarus americanus* GMGI_Hamer_2.0 GCA_018991925.1) using BWA-MEM, and host matching sequences were removed. The remaining reads were taxonomically classified with Kraken (Wood and Salzberg, 2014) against a large-scale reference database comprising all NCBI RefSeq genomes from release v205, totalling approximately 800 GB. Custom scripts were used to aggregate classification results into taxonomic profiles. Owing to the size of the reference database and datasets, analyses were performed on high memory compute nodes with 1 TB of RAM. Species- and genus-level read counts were normalised to relative abundances. Bacterial taxa were selected for visualisation if their mean relative abundance was ≥1% in at least one storage time point; for the selected taxa, mean relative abundance was reported for all storage times, and remaining low-abundance taxa grouped as 'Other'. Stacked bar plots of mean relative abundance per storage day were generated at both genus and species levels. Differential abundance analysis at the species level was performed using ANCOM-BC2 (Lin and Peddada, 2024). Species were filtered to retain those with ≥10 counts in at least two samples. Structural zero detection and bias correction were enabled. Global and pairwise tests were conducted across storage time points, and p-values were adjusted using the Benjamini–Hochberg method. Species with adjusted q-values <0.05 were considered significantly differentially abundant. Heatmaps were generated using *pheatmap* for the top 50 significant species ranked by smallest adjusted q-values. Relative abundance values were log10-transformed and z-score normalised per species prior to visualisation. Samples were ordered by storage time without column clustering to preserve temporal ordering.

3. Results

3.1. Effect of ice storage on sensory quality, nucleotide degradation and muscle pH of N. norvegicus

Quality deterioration and onset of spoilage of *N. norvegicus* during ice storage were followed through changes in QIM score, K-value and tail muscle pH (Fig. 1). QIM scores of raw whole animals significantly increased with storage time, from very low scores at the beginning of storage to the highest scores at day 16 (Kruskal-Wallis, $p = 1.8e\text{-}7$; Fig. 1A), with QIM on day 1 being significantly lower than at all subsequent sampling points and most later days also differing from each other (pairwise Wilcoxon tests, $p \leq 0.026$; Supplementary Table S2). K-values of tail muscle ATP catabolites showed a similar pattern, increasing from low initial values at day 0 to the highest values at day 16 (Kruskal-Wallis, $p = 2.9e\text{-}7$; Fig. 1B), with day 0 differing significantly from all later days and early storage (days 1-3) generally lower than days ≥7 (pairwise Wilcoxon tests, $p < 0.05$; Supplementary Table S2). Muscle pH also rose during storage, from values close to neutrality at day 0-1 to markedly higher values after 10-16 days on ice (Kruskal-Wallis, $p = 7.70e{-}9$; Fig. 1C), with significant increases from day 3 onwards and numerous differences between successive later sampling points (pairwise Wilcoxon tests, $p < 0.05$; Supplementary Table S2). According to the QIM scheme applied in this study, scores reached the rejection limit by day 7, indicating that *N. norvegicus* tails became sensorially unacceptable from this point onwards despite continued storage on ice. Together, these physicochemical and sensory changes are consistent with progressive spoilage of *N. norvegicus* tail meat during ice storage.

3.2. Culture-dependent bacterial load and characterisation of spoilage bacteria during ice storage of N. norvegicus tail muscle

Culture-based analyses showed a clear increase in bacterial load in tail muscle during storage in ice (Fig. 2). Total viable counts (TVC) remained low during the early storage period, with mean values below 4 $\log_{10}$ cfu g^{-1} from day 0 to day 5, followed by a marked increase at later time points. From day 7 onwards, TVC reached approximately 5-6 $\log_{10}$ cfu g^{-1} and remained at this level until day 16. Storage time had a highly significant effect on TVC (Fig. 2A). Pairwise comparisons showed that bacterial counts at days 7, 10, 13 and 16 were significantly higher than those observed during the early storage period (days 0-5; $p < 0.05$; Supplementary Table S2), indicating a pronounced lag phase in bacterial growth during the first days on ice, followed by rapid proliferation. Culture-dependent characterisation of spoilage bacteria was performed using a combination of MALDI-TOF MS and 16S rRNA gene Sanger sequencing on colonies isolated from tail muscle samples collected at different storage times. For the subset of colonies recovered from day-5 muscle samples and analysed by MALDI-TOF MS (n = 32), most isolates were identified as *Pseudoalteromonas nigrifaciens*, with smaller proportions assigned to *Photobacterium aquimaris* and *Psychrobacter fozii*; the remaining isolates yielded unreliable species-level identifications (Fig. 2B). Analysis of the same isolates by 16S rRNA gene Sanger sequencing supported these findings at the genus level, with *Pseudoalteromonas* predominating, followed by *Photobacterium* and *Psychrobacter* (Fig. 2C). At this timepoint, culture-based methods recovered a limited diversity within the culturable fraction of the muscle microbiota.

3.3. DNA-based quantification of bacterial load and temporal dynamics of the muscle microbiome during ice storage

DNA-based analyses revealed pronounced temporal changes in the bacterial community associated with *N. norvegicus* tail muscle during ice storage (Fig. 3). Quantitative PCR of bacterial 16S rRNA gene copy number showed that values remained close to 3 $\log_{10}$ copies per ng of DNA during the first 5 days of storage and then increased steadily, reaching approximately 4.2-4.9 $\log_{10}$ copies per ng DNA from day 7 onwards. Storage time had a highly significant effect on 16S rRNA gene copy number (ANOVA, $p = 4.9 \times 10^{-14}$; Fig. 3A), with samples from days 7 to 16 showing significantly higher values than those from days 0-5 ($p < 0.05$; Supplementary Table S2).

The tail muscle-associated bacterial community (spoilage microbiome) also changed significantly during storage on ice, as characterised by 16S rRNA gene amplicon sequencing (Fig. 3B–D). ACE richness

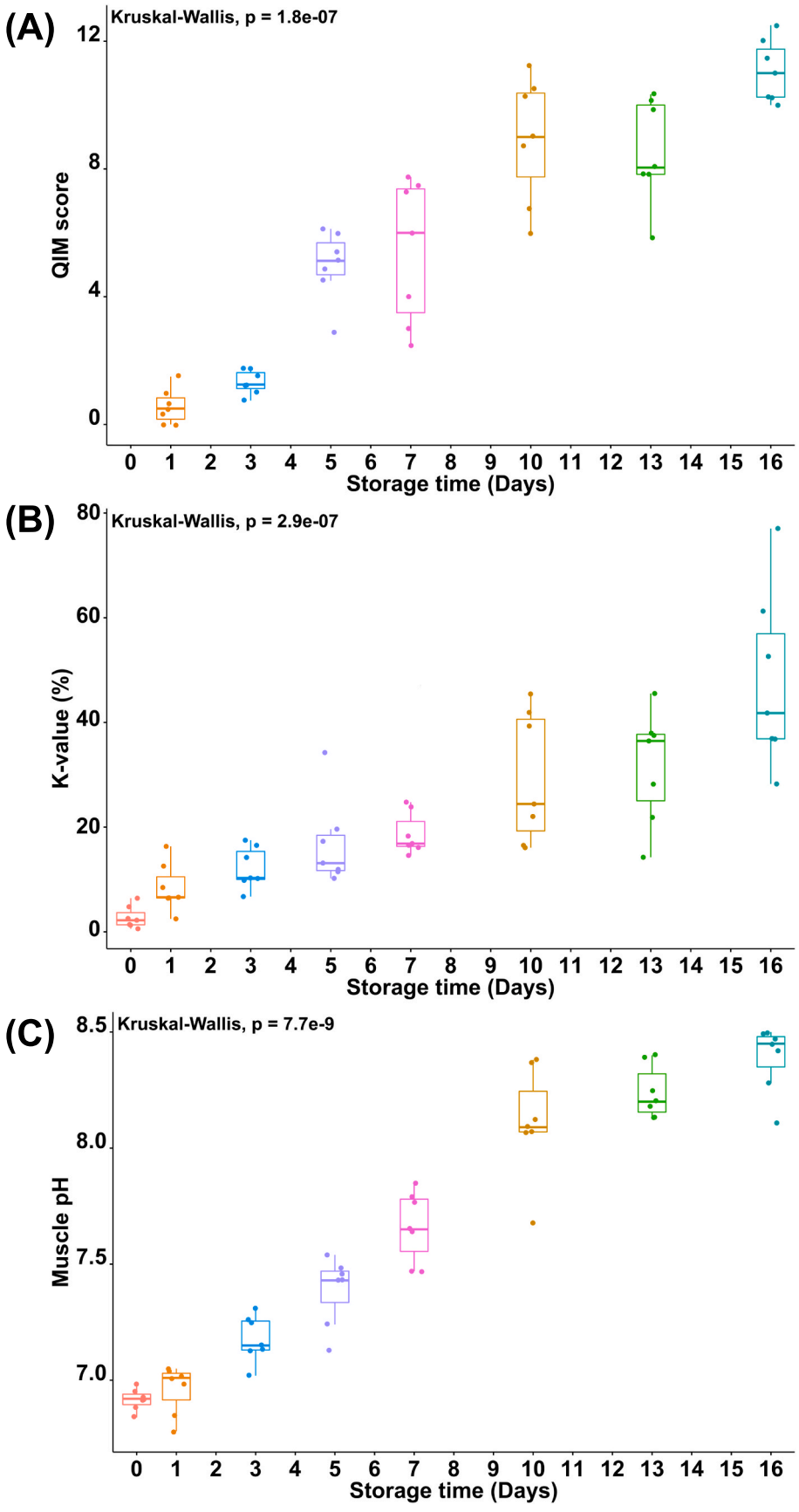

(caption on next page)

Fig. 1. Changes in sensory quality, nucleotide degradation and muscle pH of *Nephrops norvegicus* stored on ice for 16 days. Animals were stored on ice and sampled on days 0, 1, 3, 5, 7, 10, 13 and 16. (A) QIM scores are based on sensory assessment of raw whole animals. (B) K-value (%) in tail muscle, expressing the proportion of inosine 5′-monophosphate (IMP), inosine (HxR) and hypoxanthine (Hx) in total ATP-related compounds. (C) Tail muscle pH. Each dot represents an individual sample (n = 7 per sampling day). Storage time had a significant effect on all three variables (QIM: Kruskal-Wallis, $p = 1.8e{-}07$; K-value: $p = 2.9e{-}07$; pH: $p = 7.7e{-}09$), indicating progressive loss of freshness and onset of spoilage during ice storage.

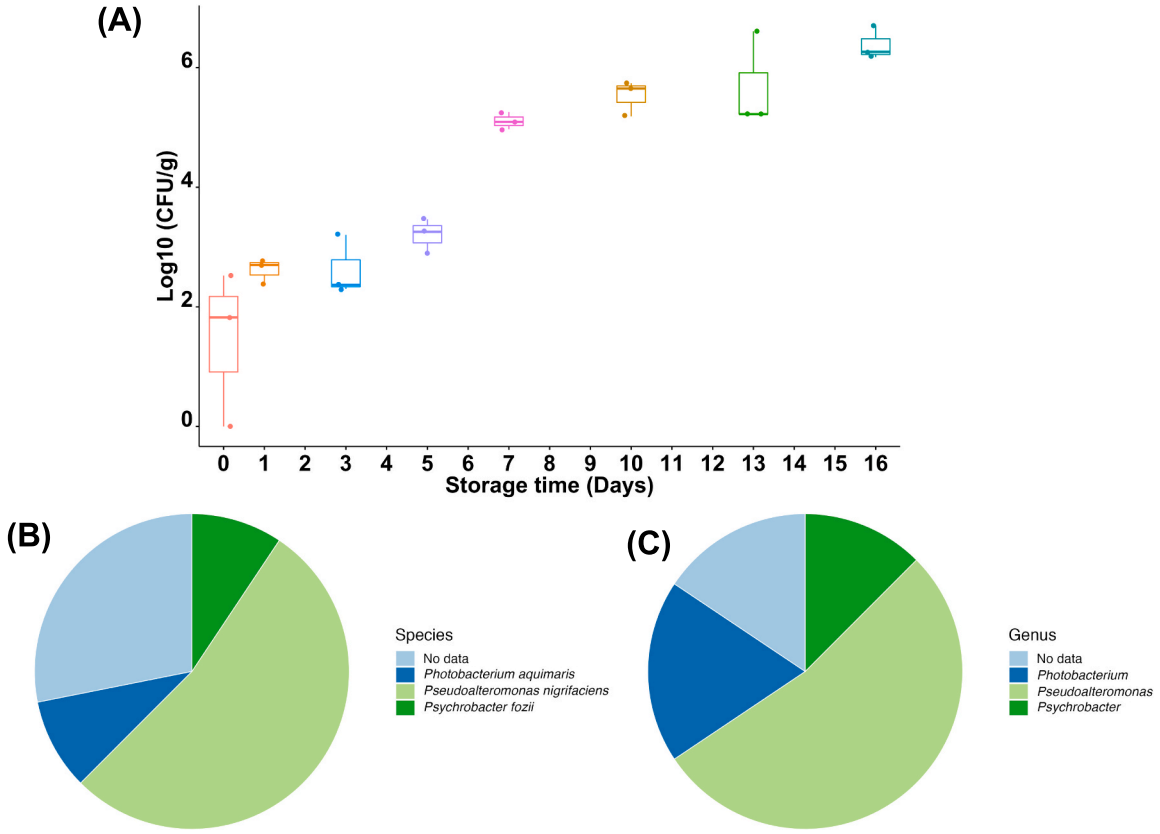

Fig. 2. Culture-dependent assessment of bacterial load and spoilage-associated bacteria in *Nephrops norvegicus* tail muscle during storage on ice. (A) Total viable counts (TVC; $\log_{10}$ cfu g^{-1}) in tail muscle during 16 days of ice storage. TVC remained low during the early storage period before increasing markedly from day 7 onwards, consistent with a pronounced lag phase followed by rapid bacterial proliferation at later storage stages. Each dot represents an individual sample (n = 3 per storage time). (B) Relative abundance of culturable bacterial species isolated from day-5 tail muscle samples and identified at species level by MALDI-TOF MS (n = 32 isolates). (C) Genus-level identification of the same day-5 isolates shown in (B), based on 16S rRNA gene Sanger sequencing. The culturable fraction was dominated by *Pseudoalteromonas*, followed by *Photobacterium* and *Psychrobacter*; remaining isolates could not be reliably assigned.

differed among storage times (ANOVA, $p = 0.013$; Fig. 3B), with day-5 samples showing significantly lower ACE values than days 0 and 1 and several later time points (days 9, 12 and 16; $p < 0.05$; Supplementary Table S3). Shannon diversity varied significantly with storage day (Kruskal-Wallis, $p = 8.3e{-}6$; Fig. 3C), with samples from days 0-3 exhibiting higher Shannon indices than those from days 5-16 ($p = 0.004$; Supplementary Table S3), whereas differences among later storage times were not significant.

Community composition (β-diversity), based on Bray-Curtis dissimilarities, was also significantly structured by storage time (PERMANOVA, $p = 0.001$; Fig. 3D). Pairwise PERMANOVA showed that communities from days 0, 1 and 3 did not differ significantly from each other ($p \geq 0.21$; Supplementary Table S3) but differed significantly from communities sampled on days 5-16 ($p \leq 0.025$ for all comparisons). In contrast, no significant differences were detected among communities from days 7, 10, 13 and 16 ($p \geq 0.21$; Supplementary Table S3), while day-5 communities showed an intermediate pattern, being not significantly different from day 7 ($p = 0.054$) but significantly different from days 10, 13 and 16 ($p \leq 0.025$; Supplementary Table S3). In the PCoA based on Bray-Curtis distances, samples from days 0-3 formed a distinct cluster, whereas samples from days 7-16 grouped in a separate region of the ordination space. Day-5 samples occupied an intermediate position between these two clusters, consistent with a transition in muscle-associated community structure and the establishment of a characteristic spoilage assemblage around this time point (Fig. 3D).

3.4. Taxonomic shifts in the muscle microbiome during ice storage

The taxonomic composition of the muscle microbiome changed markedly over the 16 days of storage on ice, based on 16S rRNA gene amplicon sequencing (Fig. 4). At the phylum level, early samples (days 0-3) were dominated by *Proteobacteria* (47-69%), but also contained substantial proportions of *Bacteroidetes* (21-39%) and lower contributions from *Fusobacteria*, *Firmicutes* and several other phyla (Supplementary Table S4, Fig. 4A). From day 5 onwards, *Proteobacteria* became overwhelmingly dominant, accounting for >97% of the community at all later time points, while *Bacteroidetes* and the remaining phyla declined to collectively <2% (Supplementary Table S4, Fig. 4A). Genus-level profiles reflected this transition from a relatively diverse early community to a *Proteobacteria*-dominated assemblage (Fig. 4B). At days 0-3, the community comprised a mixture of *unclassified Bacteroidetes/Bacteroidia* and *Saprospiraceae*, *Cocleimonas*, *Portibacter*, *Agarivorans*, *Psychrilyobacter*, *Pseudoalteromonas*, *Moritella*, *Rhodobacteraceae* and other *unclassified Gammaproteobacteria*, consistent with a

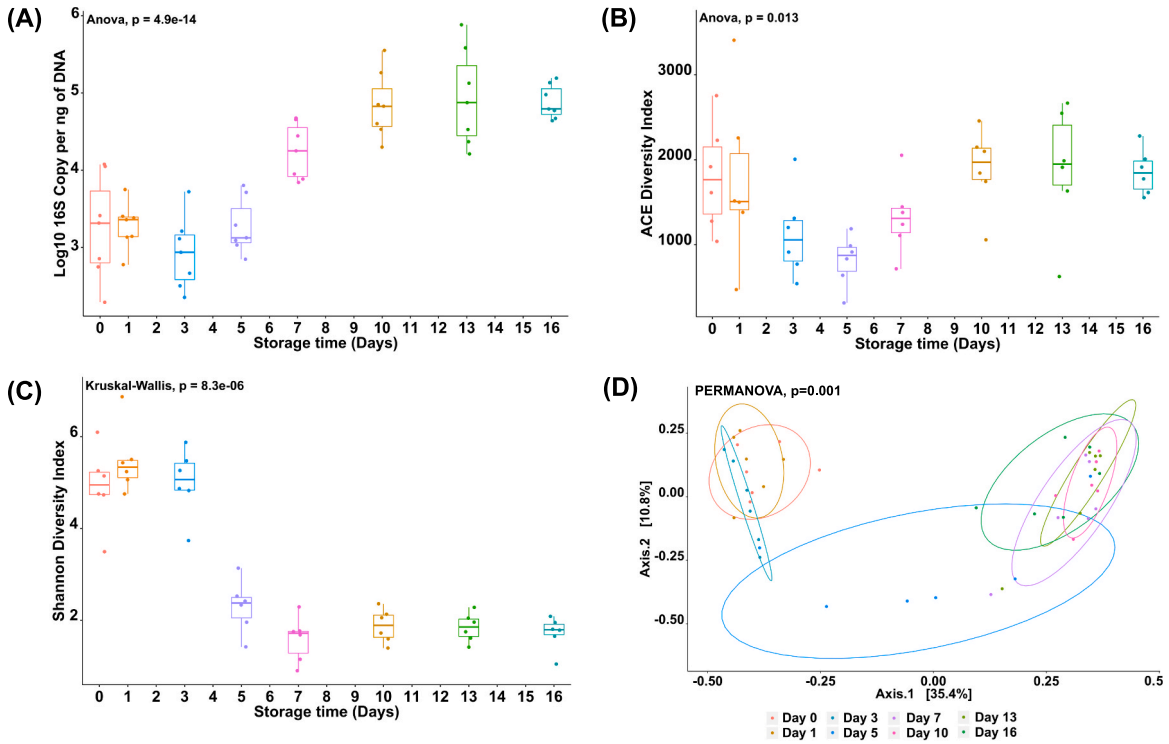

Fig. 3. DNA-based quantification of bacterial load and temporal changes in the tail muscle microbiome of *Nephrops norvegicus* during storage on ice. (A) Bacterial 16S rRNA gene copy number per ng of DNA in tail muscle. Each dot represents an individual sample (n = 7 per storage time). Storage time had a highly significant effect (ANOVA, $p = 4.9e{-}14$). (B) ACE richness and (C) Shannon diversity of bacterial communities associated with tail muscle, showing significant differences over storage time (ACE: ANOVA, $p = 0.013$; Shannon: Kruskal-Wallis, $p = 8.3e{-}06$). (D) Principal Coordinates Analysis (PCoA) based on Bray-Curtis dissimilarities, showing separation of bacterial communities by storage time (PERMANOVA, $p = 0.001$). Samples from days 0-3 cluster together, samples from days 7-16 form a separate cluster, and day-5 samples occupy an intermediate position between these groups, indicating a transition in community structure around this time point. Each dot represents an individual sample.

community reflecting the natural habitat of the animals. From day 5 onwards, psychrophilic *Gammaproteobacteria* became predominant: the putative spoilage genus *Moritella* increased from 3.4 to 6.7% at days 0-3 to 48.1% at day 5 and 44.8-69.5% at days 7-16, while *Pseudoalteromonas* rose from 1.5 to 12.6% early in storage to ~19-27% at later time points. *Aliivibrio* and *unclassified Vibrionaceae* also increased over time, from ≤1.6% to 0.5-3.8% at days 0-3 to 2.1-19.6% and 1.99-13.6%, respectively, between days 5 and 16 (Supplementary Table S5). Numerous genera showed significant differences between early (day 0) and later time points (days 5, 7 and 16), including increases in *Moritella* and *Pseudoalteromonas* and decreases in *Bacteroidetes*-affiliated and other early-community taxa such as *unclassified Bacteroidia*, *Saprospiraceae*, *Cocleimonas*, *Agarivorans* and *Psychrilyobacter* (Wilcoxon tests, BH-adjusted $p < 0.05$; Supplementary Tables S6–S10). These taxonomic shifts indicate the progressive replacement of an early, more diverse community by a *Proteobacteria*-rich spoilage microbiome dominated by *Moritella*, *Aliivibrio*, *Pseudoalteromonas* and *Vibrionaceae*.

3.5. Metagenomic profiling of the Nephrops spoilage microbiome during ice storage

Shotgun metagenomic sequencing of tail muscle at three representative storage stages (Day 0, Day 7 and Day 16) revealed a pronounced temporal restructuring of the spoilage microbiome, shifting from a highly diverse "background" community at landing to a spoilage-enriched assemblage dominated by psychrotrophic *Gammaproteobacteria* at late storage (Fig. 5). At the genus level, a large fraction of taxa at Day 0 was distributed among low-abundance genera ("Other"; 62.6%), with the most abundant named genera including *Bacteroides* (6.04%), *Pseudomonas* (4.9%), *Streptomyces* (4.4%), *Micromonospora* (3.08%) and *Thiofilum* (2.9%). By Day 7, the community exhibited a clear spoilage-associated shift, characterised by strong enrichment of *Moritella* (15.8%) and *Pseudoalteromonas* (9.2%), alongside smaller increases in *Psychrobacter* (2.38%) and *Aliivibrio* (0.66%). By Day 16, spoilage-associated genera dominated the community, with *Pseudoalteromonas* and *Aliivibrio* becoming the most abundant genera (21.7% and 20.2%, respectively), while *Moritella* remained highly abundant (12.7%) and *Photobacterium* increased substantially (5.5%) (Fig. 5A; Supplementary Table S11). Species-level profiles refined these patterns and identified a limited number of taxa driving mid-to late-stage dominance. *Pseudoalteromonas* increased from 0.14% at Day 0 to 6.83% at Day 7 and 16.55% at Day 16, while *Moritella marina* rose from near absence at Day 0 (0.013%) to 9.49% at Day 7 and remained elevated at Day 16 (7.37%). Multiple *Aliivibrio* taxa expanded during storage, with *Aliivibrio* spp. increasing from 0.004% at Day 0 to 0.18% at Day 7 and 9.28% at Day 16, alongside the emergence of *Aliivibrio logei*, *Aliivibrio sp. EL58* and *Aliivibrio sp. SR45-2* at Day 16 (3.44%, 1.56% and 1.04%, respectively). *Photobacterium* lineages also became prominent at late storage, with *Photobacterium profundum* and *P. profundum SS9* increasing to approximately 1-1.6% by Day 16 (Fig. 5B; Supplementary Table S12).

Differential abundance testing using ANCOM-BC2 identified extensive temporal restructuring of the spoilage microbiome, with 600 bacterial species exhibiting significant changes in abundance across storage time points (global $q < 0.05$; Supplementary Table S13). Enrichment was dominated by key spoilage-associated taxa belonging primarily to psychrotrophic *Gammaproteobacteria*, including multiple members of the genus *Moritella* (*Moritella* spp., *M. dasanensis ArB 0140*, *M. marina*, *Moritella sp. 24*, *Moritella sp. JT01*, *Moritella sp. PE36*, *Moritella sp. Ureatrap-13* and *M. viscosa*), *Pseudoalteromonas* (*Pseudoalteromonas* spp., *P. nigrifaciens*, *Pseudoalteromonas sp. MIP2626* and *P. translucida*), *Photobacterium* (*P. indicum* and *P. profundum*), and Aliivibrio (*Aliivibrio* spp., *A. logei*, *A. finisterrensis*, *A. fischeri* and *Aliivibrio sp. EL58*), *Psychrobacter*

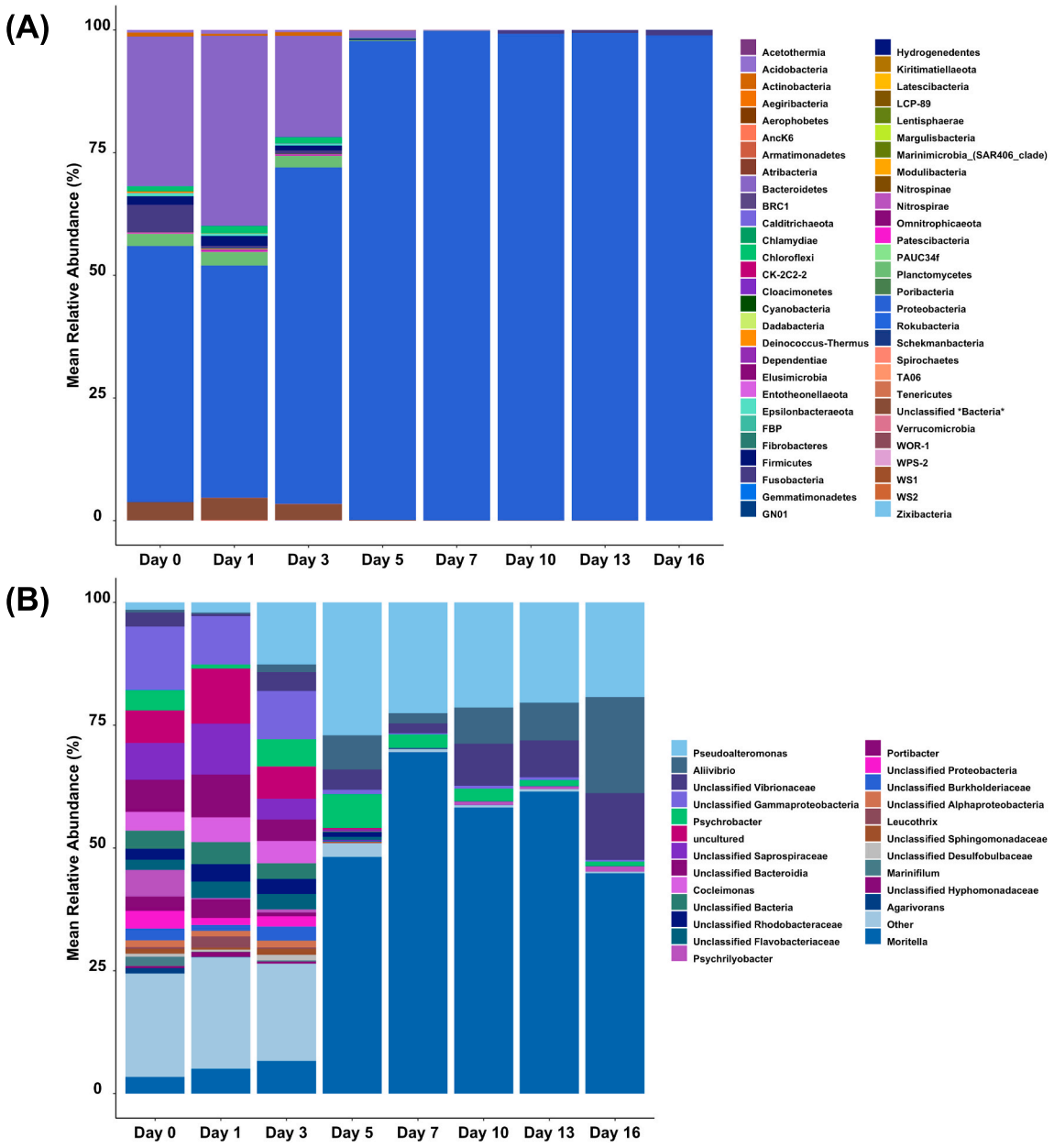

Fig. 4. Mean relative abundance of prevalent bacterial phyla and genera in the tail muscle of *Nephrops norvegicus* stored on ice for 16 days. Mean relative abundance (%) of bacterial taxa in tail muscle samples (n = 6 per time point). (A) Mean relative abundance at the phylum level. (B) Mean relative abundance at genus level; bacterial genera with an overall abundance >1% are shown individually, while taxa with an abundance <1% were pooled and are indicated as "Others". The plots illustrate the shift from a diverse early community to a *Proteobacteria*-dominated spoilage assemblage.

(*Psychrobacter* spp. and *P. immobilis*) and *Shewanella hanedai* (all $q < 0.05$; Supplementary Table S13). Heatmap visualisation of the top differentially abundant species (ranked by smallest global q-values; $q < 0.05$) revealed clear temporal structuring of the microbiome, with Day 0 samples separating from those collected at Days 7 and 16, and mid-to late-stage storage characterised by coordinated increases in *Pseudoalteromonas*, *Moritella*, *Aliivibrio* and *Photobacterium* clades (Fig. 5C).

4. Discussion

The combined progression of sensory quality, nucleotide degradation and muscle pH observed in this study reflects a differential quality loss trajectory, with autolytic-driven measures increasing from day 1 onwards (K-value), muscle pH and QIM values having a relatively short lag phase (1-3 days) and microbial abundance and composition changing after a relatively long lag phase (day 5-7). Sensory rejection, as defined by the QIM score (5.4), was reached by day 7 and coincided with pronounced increases in K-value (18.7%) and muscle pH (7.6). Importantly, the convergence of these quality indices around days 5-7 highlights the presence of a critical "tipping point" for spoilage development. This transition point coincided with the onset of rapid bacterial proliferation and restructuring of the muscle microbiome, consistent with the broader view that sensory rejection is driven by the combined effects of autolysis and microbial metabolism (Gram and Huss, 1996). Notably, sensory rejection also coincided with the emergence of a psychrotrophic spoilage-associated assemblage, indicating that spoilage development was associated not only with increasing bacterial biomass, but also with shifts in community structure and activity. The transition observed between days 5 and 7 suggests that the activity of these taxa and the

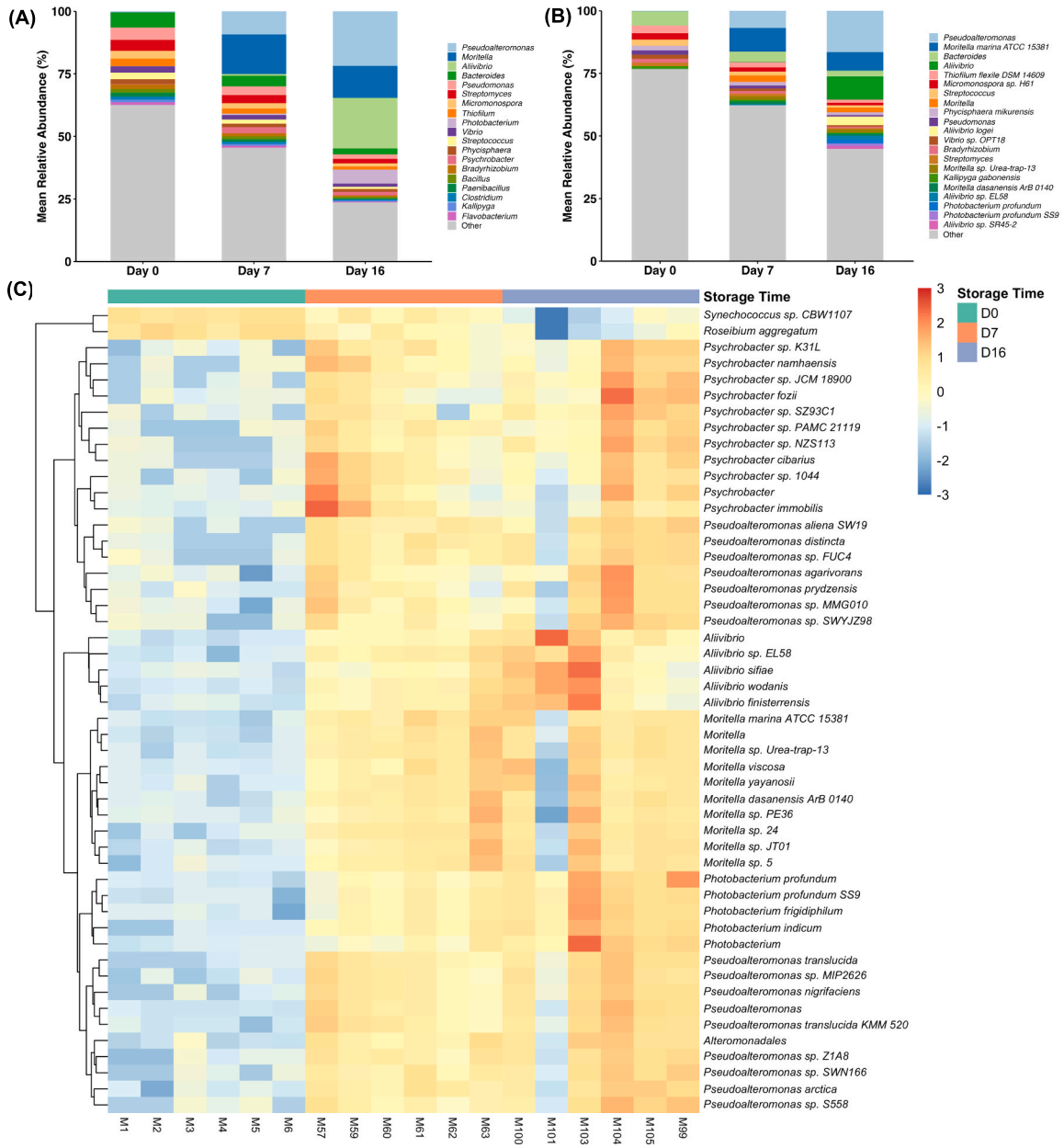

Fig. 5. Metagenomic profiling of the spoilage microbiome in *Nephrops norvegicus* tail muscle during ice storage. (A) Genus-level mean relative abundance of bacterial taxa contributing ≥1% within at least one storage time point (D0, D7, D16). Genera with lower relative abundance are grouped as "Other". (B) Species-level mean relative abundance of bacterial taxa contributing ≥1% within at least one storage time point, with remaining species grouped as "Other". (C) Heatmap of the top 50 bacterial species showing the strongest significant association with storage time based on ANCOM-BC2 global testing ($q < 0.05$), ranked by smallest q-values. Relative abundances were log-transformed and z-score normalised per species. Samples are ordered by storage time (D0, D7, D16). Colour intensity indicates standardised relative abundance, with red representing higher and blue lower abundance relative to the species mean. (For interpretation of the references to colour in this figure legend, the reader is referred to the Web version of this article.)

production of spoilage-associated bacterial metabolites, together with endogenous post-mortem degradation processes, contributed to sensory deterioration during ice storage. As such, this mid-storage phase provides a biologically meaningful framework for understanding subsequent microbial succession and identifies a practical window for quality management and shelf-life optimisation under conventional icing conditions.

Culture-based enumeration showed a pronounced lag phase, with TVC remaining below ~4 $\log_{10}$ cfu g^{-1} until day 5 before increasing sharply from day 7 onwards. Counts below this threshold are commonly considered indicative of fresh fish (Zheng et al., 2020). However, in cold-water fish products, TVC values tend to increase linearly throughout storage or exhibit shorter lag phases under icing conditions (Fogarty et al., 2019; Zheng et al., 2020), rather than the extended lag phase observed here. A similar lag phase during iced storage has been reported for *N. norvegicus* tail muscle using culture-based methods (Albalat et al., 2011). This lag phase indicates a strong temperature-driven selection and the time required for psychrotolerant bacteria to adapt to and exploit available substrates under cold storage conditions, which would seem to be particularly long in this type of product. The temporal pattern observed using culture-based enumeration was closely mirrored by absolute quantification of bacterial 16S rRNA gene copy number, with both approaches identifying a pronounced increase in bacterial biomass from day 7 onwards. While total viable counts capture only the culturable fraction of the bacteria, 16S rRNA gene quantification reflects total bacterial DNA and therefore

encompasses both culturable and non-culturable bacteria. The strong alignment between these methods in the present study supports the continued relevance of the conventional plate counts while highlighting 16S rRNA gene quantification as a robust quantitative indicator of microbial load. Amplicon sequencing profiles primarily resolved changes in community composition rather than absolute abundance, while normalisation of amplicon libraries using absolute 16S rRNA gene copy numbers enabled more consistent comparison of microbial succession across samples.

Culturable bacteria isolated from *N. norvegicus* tail muscle during ice storage were dominated by the genera *Pseudoalteromonas*, *Photobacterium* and *Psychrobacter*. These taxa are commonly associated with cold marine environments and frequently form part of spoilage microbial communities in chilled fish and shellfish products (Antunes-Rohling et al., 2019; Sequino et al., 2024). Their recovery is consistent with previous culture-based studies, which have identified them among the dominant culturable bacteria during spoilage trials in this species (Broekaert et al., 2011; Gornik et al., 2013). *Photobacterium* includes well-recognised specific spoilage organisms in chilled seafood, and *Pseudoalteromonas* and *Psychrobacter* are more commonly associated with early to mid-stage spoilage communities.

The relatively limited diversity recovered by culture-based methods at day 5, compared with the broader diversity revealed by 16S rRNA gene amplicon sequencing, reflects the inherent selectivity of plate-based recovery, which favours fast-growing and readily culturable organisms (Amann et al., 1995). Similar limitations of culture-based approaches in resolving the full complexity of seafood microbiomes have been highlighted previously, with selective recovery often biasing detection towards dominant taxa (Doulgeraki and Nychas, 2013). This discrepancy between culture-dependent and sequencing-based profiles highlights the complementary nature of these approaches. While high-throughput sequencing provides a more comprehensive view of community composition, culture-based methods remain essential for identifying viable bacteria that are most likely to contribute directly to spoilage-related sensory deterioration (Reynisson et al., 2009). Together, these approaches provide a more ecologically meaningful understanding of spoilage processes.

Sequencing-based analyses further contextualised spoilage development in *N. norvegicus* tail muscle by revealing a clear microbial successional pattern during ice storage. The fresh muscle microbiome was initially characterised by high taxonomic diversity, comprising taxa commonly associated with marine sediments and seawater, consistent with the natural habitat of the animals (Hoshino et al., 2020). This diverse assemblage was maintained during early storage (days 0-3); however, a pronounced restructuring occurred between days 5 and 7, coinciding with sensory rejection and a sharp increase in bacterial biomass. During this transition, alpha diversity declined markedly, and community composition shifted towards dominance by a limited number of psychrophilic *Gammaproteobacteria*, reflecting strong selective pressures imposed by low temperature and substrate availability. Such reductions in diversity and convergence towards dominant psychrotrophic taxa are widely observed during fish and seafood spoilage (Sequino et al., 2022). From day 5 onwards, the muscle microbiome became dominated by *Moritella*, together with increased contributions from *Aliivibrio*, unclassified *Vibrionaceae, Psychrobacter,* and *Pseudoalteromonas*, defining a distinct spoilage assemblage. The prominence of *Moritella* is particularly noteworthy, as this genus has emerged in recent years as an important contributor to spoilage signatures in chilled marine fish, including *Scomber scombrus* (Piredda et al., 2023), *Merluccius merluccius* (Antunes-Rohling et al., 2019) and *Trachurus japonicus* (Kyoui et al., 2022), despite its limited representation in traditional culture-based spoilage studies.

The integration of amplicon sequencing with metagenomics is increasingly recognised as a powerful strategy in food microbiology, enabling both robust taxonomic profiling and inference of functional potential within microbial communities (Sequino et al., 2022). Recent studies show that integrating microbiological and molecular datasets provides a more comprehensive understanding of seafood spoilage than single-method approaches (Lytou et al., 2024). A key outcome of this study is the strong agreement between 16S rRNA gene amplicon sequencing and shotgun metagenomics at the genus level, with both approaches identifying *Moritella*, *Pseudoalteromonas*, *Aliivibrio* and *Photobacterium* as the dominant taxa associated with mid-to late-stage spoilage. This concordance indicates that amplicon sequencing reliably captures the principal microbial shifts underlying spoilage development during ice storage. Owing to its lower cost, analytical simplicity and suitability for high sample throughput, 16S rRNA gene amplicon sequencing represents a practical and scalable approach for routine spoilage monitoring, shelf-life evaluation and comparative storage trials in crustacean products, while shotgun metagenomics provides added value when species-level resolution or targeted mechanistic insight is required.

The spoilage of ice-stored *N. norvegicus* muscle was associated with the co-enrichment of a defined species-level bacterial consortium. This assemblage was dominated by multiple taxa, including several *Moritella* species (*M. marina*, *M. dasanensis* and *M. viscosa*), *Aliivibrio* spp. (e.g. *A. logei*, *A. finisterrensis* and *A. fischeri*), *Pseudoalteromonas* spp. (notably *P. nigrifaciens* and *P. translucida*), and *Photobacterium* lineages (*P. profundum* and *P. indicum*), with additional contributions from *Shewanella hanedai, Alteromonadales* spp. and *Psychrobacter immobilis*. *Moritella* species (*M. marina*, *M. viscosa* and *M. dasanensis*) formed a core component of this assemblage. However, dominance within the spoilage microbiome alone does not define a specific spoilage organism (SSO), as spoilage activity depends on the production of metabolites directly associated with sensory deterioration. The consistent enrichment of *Moritella* during the spoilage transition observed here, together with its increasing recognition in sequencing-based studies of chilled marine fish spoilage (Antunes-Rohling et al., 2019; Kyoui et al., 2022; Piredda et al., 2023), supports its potential role as a spoilage-associated taxon in this product. Nevertheless, *Moritella* remains underrepresented in traditional isolation-based spoilage studies, which may partly reflect the specialised growth requirements of psychrophilic marine bacteria and limitations of conventional culture conditions. Direct functional validation linking *Moritella* to specific spoilage metabolite production in *N. norvegicus* is still required before it can be definitively considered a specific spoilage organism.

M. viscosa is a psychrophilic marine bacterium recognised as the primary agent of winter ulcer disease in cold-water fish (Løvoll et al., 2009). *M. marina* and *M. dasanensis* are also psychrophilic marine bacteria originally described from cold marine habitats (Kim et al., 2008), consistent with taxa capable of growth at low temperatures. Although these species have not been widely reported as established seafood spoilage organisms, they are phylogenetically related to recognised spoilage-associated genera such as *Shewanella* and *Pseudoalteromonas* (Urakawa et al., 1998), supporting their potential involvement in spoilage processes under chilled storage, although direct functional contributions in *N. norvegicus* muscle spoilage remain to be established. *A. logei*, *A. fischeri* and *A. finisterrensis* are cold-adapted marine bacteria associated with aquatic animals, and recent multi-omics studies of chilled seafood have linked *Aliivibrio* spp. to spoilage-related volatile organic compounds and sensory deterioration, supporting their potential involvement in spoilage processes (Macé et al., 2025). *Photobacterium* lineages, including *P. profundum* and *P. indicum*, have previously been linked to spoilage in chilled marine products through trimethylamine oxide reduction and the generation of off-odours (Gornik et al., 2011; Rolin et al., 2023). The enrichment of *Pseudoalteromonas* spp. and *P. immobilis* is consistent with previous spoilage studies in crustacean matrices (Bekaert et al., 2015; K. Broekaert et al., 2013), where these genera are frequently detected and have been shown to possess lipolytic and proteolytic capacities and to produce spoilage-relevant volatile profiles (Katrie Broekaert et al., 2013). Although *S. hanedai* and *Alteromonadales* spp. were not dominant

members of the community, their detection among differentially abundant taxa is compatible with the well-established role of *Shewanella* and related marine *Gammaproteobacteria* as contributors to seafood spoilage through the production of sulphur compounds, trimethylamine and dimethylamine under chilled storage (Boziaris and Parlapani, 2017; Kyoui et al., 2022; Odeyemi et al., 2018). Together, these findings indicate that spoilage of ice-stored *N. norvegicus* muscle reflects the collective activity of a structured multi-species consortium rather than the dominance of a single organism. Resolving this assemblage at species level refines current understanding of *Nephrops* spoilage ecology and highlights the importance of considering spoilage as a community-level process when designing shelf-life extension strategies for crustacean products. Future studies integrating metabolomics or targeted functional assays will be important to directly link microbial taxa to the production of specific spoilage-associated metabolites. In addition, assessing the effects of storage temperature, handling conditions and catch-to-catch variability will help determine the stability of the identified spoilage consortium across different storage scenarios.

In conclusion, this study defines a critical mid-storage transition (days 5-7) in ice-stored *N. norvegicus* in which sensory rejection coincides with a sharp rise in bacterial biomass and establishment of a stable spoilage assemblage. The strong concordance between 16S amplicon sequencing and metagenomics at genus level supports amplicon profiling as a practical, scalable approach for shelf-life monitoring, while species-level metagenomic resolution highlights a structured consortium comprising *Moritella* spp., *Aliivibrio* spp., *Pseudoalteromonas* spp. and *Photobacterium* lineages, alongside lower-abundance contributors including *Shewanella* and *Psychrobacter*. These findings provide a high-resolution assessment of spoilage development and open avenues for targeted interventions aimed at shelf-life extension, including bacteriophage-based biocontrol approaches directed against dominant psychrotrophic spoilage-associated taxa identified during spoilage progression.

Funding sources

This study was funded by the UK Seafood Innovation Fund administered by the Centre for Environment Fisheries and Aquaculture Science (Cefas) on behalf of the Department for Environment Farming and Rural Affairs (Defra), SIF3 Feasibility Study, project code FS155.

CRediT authorship contribution statement

Ahmed Elsheshtawy: Conceptualization, Data curation, Formal analysis, Investigation, Methodology, Software, Validation, Visualization, Writing – original draft. **Benjamin G.J. Clokie:** Conceptualization, Formal analysis, Funding acquisition, Investigation, Methodology, Supervision, Validation, Writing – review & editing. **Sasha Saugh:** Formal analysis, Investigation, Methodology. **Karen D. Adler:** Formal analysis, Methodology, Writing – review & editing. **Slawomir M. Michniewski:** Formal analysis, Methodology, Writing – review & editing. **Simon MacKenzie:** Conceptualization, Investigation, Methodology, Resources, Supervision, Writing – review & editing. **Martha R.J. Clokie:** Conceptualization, Formal analysis, Funding acquisition, Investigation, Methodology, Project administration, Supervision, Validation, Writing – review & editing. **Thomas Sicheritz-Pontén:** Conceptualization, Data curation, Formal analysis, Methodology, Resources, Software, Validation, Writing – review & editing. **Amaya Albalat:** Conceptualization, Formal analysis, Funding acquisition, Investigation, Methodology, Project administration, Supervision, Validation, Writing – review & editing.

Declaration of competing interest

The authors declare that they have no known competing financial interests or personal relationships that could have appeared to influence the work reported in this paper.

Acknowledgements

The authors are grateful to skipper Mr Ian Wightman for his assistance and cooperation in sourcing the fresh specimens used in this study.

Appendix A. Supplementary data

Supplementary data to this article can be found online at https://doi.org/10.1016/j.fm.2026.105151.

Data availability

The datasets generated and analysed during this study are available in online repositories under SRA submission number PRJNA1403385.

References

Albalat, A., Gornik, S.G., Atkinson, R.J.A., Coombs, G.H., Neil, D.M., 2009. Effect of capture method on the physiology and nucleotide breakdown products in the Norway lobster (*Nephrops norvegicus*). Mar. Biol. Res. 5 (5), 441–450. https://doi.org/10.1080/17451000802603637.

Albalat, A., Gornik, S.G., Mullen, W., Crozier, A., Atkinson, R.J.A., Coombs, G.H., Neil, D. M., 2011. Quality changes in chilled Norway lobster (*Nephrops norvegicus*) tail meat and the effects of delayed icing. Int. J. Food Sci. Technol. 46 (7), 1413–1421. https://doi.org/10.1111/j.1365-2621.2011.02650.x.

Amann, R.I., Ludwig, W., Schleifer, K.H., 1995. Phylogenetic identification and in situ detection of individual microbial cells without cultivation. Microbiol. Rev. 59 (1), 143–169. https://doi.org/10.1128/mr.59.1.143-169.1995.

Anagnostopoulos, D.A., Parlapani, F.F., Boziaris, I.S., 2022. The evolution of knowledge on seafood spoilage microbiota from the 20th to the 21st century: have we finished or just begun? Trends Food Sci. Technol. 120, 236–247. https://doi.org/10.1016/j.tifs.2022.01.004.

Antunes-Rohling, A., Calero, S., Halaihel, N., Marquina, P., Raso, J., Calanche, J., Cebrián, G., 2019. Characterization of the spoilage microbiota of hake fillets packaged under a modified atmosphere (MAP) rich in CO(2) (50% CO(2)/50% N(2)) and stored at different temperatures. Foods 8 (10). https://doi.org/10.3390/foods8100489.

Artawinata, P.C., Lorraine, S., Waturangi, D.E., 2023. Isolation and characterization of bacteriophages from soil against food spoilage and foodborne pathogenic bacteria. Sci. Rep. 13 (1), 9282. https://doi.org/10.1038/s41598-023-36591-6.

Bekaert, K., Devriese, L., Maes, S., Robbens, J., 2015. Characterization of the dominant bacterial communities during storage of Norway lobster and Norway lobster tails (*Nephrops norvegicus*) based on 16S rDNA analysis by PCR-DGGE. Food Microbiol. 46, 132–138. https://doi.org/10.1016/j.fm.2014.06.022.

Benjamini, Y., Hochberg, Y., 1995. Controlling the false discovery rate: a practical and powerful approach to multiple testing. J. Roy. Stat. Soc. B 57 (1), 289–300.

Boziaris, I.S., Kordila, A., Neofitou, C., 2011. Microbial spoilage analysis and its effect on chemical changes and shelf-life of Norway lobster (*Nephrops norvegicus*) stored in air at various temperatures. Int. J. Food Sci. Technol. 46 (4), 887–895. https://doi.org/10.1111/j.1365-2621.2011.02568.x.

Boziaris, I.S., Parlapani, F.F., 2017. Chapter 3 - Specific Spoilage Organisms (SSOs) in fish. In: Bevilacqua, A., Corbo, M.R., Sinigaglia, M. (Eds.), The Microbiological Quality of Food. Woodhead Publishing, pp. 61–98. https://doi.org/10.1016/B978-0-08-100502-6.00006-6.

Broekaert, K., Heyndrickx, M., Herman, L., Devlieghere, F., Vlaemynck, G., 2011. Seafood quality analysis: molecular identification of dominant microbiota after ice storage on several general growth media. Food Microbiol. 28 (6), 1162–1169. https://doi.org/10.1016/j.fm.2011.03.009.

Broekaert, K., Heyndrickx, M., Herman, L., Devlieghere, F., Vlaemynck, G., 2013a. Molecular identification of the microbiota of peeled and unpeeled brown shrimp (*Crangon crangon*) during storage on ice and at 7.5°C. Food Microbiol. 36 (2), 123–134. https://doi.org/10.1016/j.fm.2013.04.009.

Broekaert, K., Noseda, B., Heyndrickx, M., Vlaemynck, G., Devlieghere, F., 2013b. Volatile compounds associated with Psychrobacter spp. and Pseudoalteromonas spp., the dominant microbiota of brown shrimp (*Crangon crangon*) during aerobic storage. Int. J. Food Microbiol. 166 (3), 487–493. https://doi.org/10.1016/j.ijfoodmicro.2013.08.013.

Cao, Y., Fanning, S., Proos, S., Jordan, K., Srikumar, S., 2017. A review on the applications of next generation sequencing technologies as applied to food-related microbiome studies. Front. Microbiol. 8, 1829. https://doi.org/10.3389/fmicb.2017.01829.

Chiou, T.-K., Huang, J.-P., 2004. Biochemical changes in the abdominal muscle of mud crab (*Scylla serrata*) during storage. Fish. Sci. 70 (1), 167–173. https://doi.org/10.1111/j.1444-2906.2003.00785.x.

Clokie, B.G.J., Elsheshtawy, A., Albalat, A., Nylund, A., Beveridge, A., Payne, C.J., MacKenzie, S., 2022. Optimization of low-biomass sample collection and quantitative PCR-based titration impact 16S rRNA microbiome resolution.

Microbiol. Spectr. 10 (6). https://doi.org/10.1128/smpectru.02255-22 e02255-02222.
Coates, C., Albalat, A., 2014. Engaging with strategies to impede post morte m hyperpigmentation in commercial crustaceans. Shellfish: Human Consumpt. Healt h Implicat. Conservat. Concern. 169–193.
Cocolin, L., Mataragas, M., Bourdichon, F., Doulgeraki, A., Pilet, M.-F., Jagadeesan, B., Phister, T., 2018. Next generation microbiological risk assessment meta-omics: the next need for integration. Int. J. Food Microbiol. 287, 10–17. https://doi.org/10.1016/j.ijfoodmicro.2017.11.008.
Doulgeraki, A.I., Nychas, G.-J.E., 2013. Monitoring the succession of the biota grown on a selective medium for *pseudomonads* during storage of minced beef with molecular-based methods. Food Microbiol. 34 (1), 62–69. https://doi.org/10.1016/j.fm.2012.11.017.
Elsheshtawy, A., Clokie, B.G.J., Albalat, A., Beveridge, A., Hamza, A., Ibrahim, A., MacKenzie, S., 2021. Characterization of External Mucosal Microbiomes of Nile Tilapia and Grey Mullet Co-cultured in Semi-Intensive Pond Systems [Original Research]. Front. Microbiol. 12. https://doi.org/10.3389/fmicb.2021.773860, 2021.
Elsheshtawy, A., Clokie, B.G.J., Albalat, A., Nylund, A., Isaksen, T.E., Napsøy Indrebø, E., MacKenzie, S., 2023. Net cleaning impacts Atlantic salmon gill health through microbiome dysbiosis. Front. Aquacult. 2. https://doi.org/10.3389/faquc.2023.1125595, 2023.
Fogarty, C., Whyte, P., Brunton, N., Lyng, J., Smyth, C., Fagan, J., Bolton, D., 2019. Spoilage indicator bacteria in farmed Atlantic salmon (*Salmo salar*) stored on ice for 10 days. Food Microbiol. 77, 38–42. https://doi.org/10.1016/j.fm.2018.08.001.
Gornik, S.G., Albalat, A., Macpherson, H., Birkbeck, H., Neil, D.M., 2011. The effect of temperature on the bacterial load and microbial composition in Norway lobster (*Nephrops norvegicus*) tail meat during storage. J. Appl. Microbiol. 111 (3), 582–592. https://doi.org/10.1111/j.1365-2672.2011.05081.x.
Gornik, S.G., Albalat, A., Theethakaew, C., Neil, D.M., 2013. Shelf life extension of whole Norway lobster *Nephrops norvegicus* using modified atmosphere packaging. Int. J. Food Microbiol. 167 (3), 369–377. https://doi.org/10.1016/j.ijfoodmicro.2013.10.002.
Gram, L., Dalgaard, P., 2002. Fish spoilage bacteria – problems and solutions. Curr. Opin. Biotechnol. 13 (3), 262–266. https://doi.org/10.1016/S0958-1669(02)00309-9.
Gram, L., Huss, H.H., 1996. Microbiological spoilage of fish and fish products. Int. J. Food Microbiol. 33 (1), 121–137. https://doi.org/10.1016/0168-1605(96)01134-8.
Hoshino, T., Doi, H., Uramoto, G.-I., Wörmer, L., Adhikari, R.R., Xiao, N., Inagaki, F., 2020. Global diversity of microbial communities in marine sediment. In: Proceedings of the National Academy of Sciences, 117, pp. 27587–27597. https://doi.org/10.1073/pnas.1919139117, 44.
Kassambara, A., 2020. Pipe-Friendly Framework for Basic Statistical Tests [R package rstatix version 0.6.0].
Kim, H.J., Park, S., Lee, J.M., Park, S., Jung, W., Kang, J.S., Kang, S.H., 2008. *Moritella dasanensis* sp. nov., a psychrophilic bacterium isolated from the Arctic ocean. Int. J. Syst. Evol. Microbiol. 58 (Pt 4), 817–820. https://doi.org/10.1099/ijs.0.65501-0.
Kyoui, D., Fukasawa, Y., Miyanaga, W., Nakamura, Y., Yamane, T., Sugita, K., Ogihara, H., 2022. Identification of changes in the microflora composition of Japanese horse mackerel (*Trachurus japonicus*) during storage to identify specific spoilageorganisms. Curr. Res. Food Sci. 5, 1216–1224. https://doi.org/10.1016/j.crfs.2022.07.015.
Lin, H., Peddada, S.D., 2024. Multigroup analysis of compositions of microbiomes with covariate adjustments and repeated measures. Nat. Methods 21 (1), 83–91. https://doi.org/10.1038/s41592-023-02092-7.
Løvoll, M., Wiik-Nielsen, C.R., Tunsjø, H.S., Colquhoun, D., Lunder, T., Sørum, H., Grove, S., 2009. Atlantic salmon bath challenged with *Moritella viscosa* – pathogen invasion and host response. Fish Shellfish Immunol. 26 (6), 877–884. https://doi.org/10.1016/j.fsi.2009.03.019.
Lytou, A., Saxton, L., Fengou, L.-C., Anagnostopoulos, D.A., Parlapani, F.F., Boziaris, I.S., Nychas, G.-J., 2024. Contribution of data acquired from spectroscopic, genomic and microbiological analyses to enhance mussels' quality assessment. Food Res. Int. 197, 115207. https://doi.org/10.1016/j.foodres.2024.115207.
Macé, S., Rannou, C., Jérôme, M., Chevalier, F., Kolypczuk, L., Donnay-Moreno, C., Noël, C., 2025. Multi-omics signature profiles of cold-smoked salmon from different processing plants: insights into spoilage dynamics. Int. J. Food Microbiol. 438, 111233. https://doi.org/10.1016/j.ijfoodmicro.2025.111233.
Martin, I., Elsheshtawy, A., Clokie, B.G.J., MacKenzie, S., Bateman, K.S., Bass, D., Albalat, A., 2025. Microbiome dynamics associated with Hematodinium sp. infection in Norway lobster (*Nephrops norvegicus*). Animal Microb. 7 (1), 62. https://doi.org/10.1186/s42523-025-00416-w.
Martıénez-Alvarez, O., López-Caballero, M.E., Montero, P., Gómez-Guillén, M.C., 2007. Spraying of 4-hexylresorcinol based formulations to prevent enzymatic browning in Norway lobsters (*Nephrops norvegicus*) during chilled storage. Food Chem. 100 (1), 147–155. https://doi.org/10.1016/j.foodchem.2005.09.031.
McMurdie, P.J., Holmes, S., 2013. Phyloseq: an R package for reproducible interactive analysis and graphics of microbiome census data. PLoS One 8 (4), e61217.
MMO, 2025. UK Sea Fisheries Statistics 2024, 2 December 2025 Retrieved from. https://assets.publishing.service.gov.uk/media/692db8a7345e31ab14ecf833/2025_12_02_-_UK_Sea_Fisheries_Statistics_2024_report_-_.pdf.
Odeyemi, O.A., Burke, C.M., Bolch, C.C.J., Stanley, R., 2018. Seafood spoilage microbiota and associated volatile organic compounds at different storage temperatures and packaging conditions. Int. J. Food Microbiol. 280, 87–99. https://doi.org/10.1016/j.ijfoodmicro.2017.12.029.
Odeyemi, O.A., Burke, C.M., Bolch, C.C.J., Stanley, R., 2019. Spoilage microbial community profiling by 16S rRNA amplicon sequencing of modified atmosphere packaged live mussels stored at 4°C. Food Res. Int. 121, 568–576. https://doi.org/10.1016/j.foodres.2018.12.017.
Oksanen, J., Blanchet, F.G., Kindt, R., Legendre, P., Minchin, P.R., O'hara, R., Wagner, H., 2013. Package 'vegan'. Commun. Ecol Package, version 2 (9), 1–295.
Parlapani, F.F., Ferrocino, I., Michailidou, S., Argiriou, A., Haroutounian, S.A., Kokokiris, L., Boziaris, I.S., 2020. Microbiota and volatilome profile of fresh and chill-stored deepwater rose shrimp (*Parapenaeus longirostris*). Food Res. Int. 132, 109057. https://doi.org/10.1016/j.foodres.2020.109057.
Piredda, R., Mottola, A., Lorusso, L., Ranieri, L., Catanese, G., Cipriano, G., Di Pinto, A., 2023. Microbiome-based study in wild-caught Scomber scombrus fish products at the end of the supply chain. Lebensm. Wiss. Technol. 186, 115264. https://doi.org/10.1016/j.lwt.2023.115264.
Quast, C., Pruesse, E., Yilmaz, P., Gerken, J., Schweer, T., Yarza, P., Glöckner, F.O., 2013. The SILVA ribosomal RNA gene database project: improved data processing and web-based tools. Nucleic Acids Res. 41 (D1), D590–D596. https://doi.org/10.1093/nar/gks1219.
Reynisson, E., Lauzon, H.L., Magnússon, H., Jónsdóttir, R., Olafsdóttir, G., Marteinsson, V., Hreggvidsson, G.O., 2009. Bacterial composition and succession during storage of North-Atlantic cod (*Gadus morhua*) at superchilled temperatures. BMC Microbiol. 9, 250. https://doi.org/10.1186/1471-2180-9-250.
Rolin, J., Horricks, R.A., Stephen, J., Watson, K., Clark, K.F., Lewis-McCrea, L.M., Reid, G.K., 2023. Changes in bacterial communities in chilled American lobster (*Homarus americanus*) tissues following mortality. Lebensm. Wiss. Technol. 185, 115136. https://doi.org/10.1016/j.lwt.2023.115136.
Rolle, R., Guizani, N., Chen, J., Marshall, M., Yang, J., Wei, C., 1991. Purification and characterization of phenoloxidase isoforms from Taiwanese black tiger shrimp (*Penaeus monodon*) 1. J. Food Biochem. 15 (1), 17–32.
Ryder, J.M., 1985. Determination of adenosine triphosphate and its breakdown products in fish muscle by high-performance liquid chromatography. J. Agric. Food Chem. 33 (4), 678–680. https://doi.org/10.1021/jf00064a027.
Saito, T., Arai, K.i., Matsuyoshi, M., 1959. A new method for estimating the freshness of fish. Nippon Suisan Gakkaishi 24, 749–750.
Schloss Patrick, D., Westcott Sarah, L., Ryabin, T., Hall Justine, R., Hartmann, M., Hollister Emily, B., Weber Carolyn, F., 2009. Introducing mothur: open-source, platform-independent, community-supported software for describing and comparing microbial communities. Appl. Environ. Microbiol. 75 (23), 7537–7541. https://doi.org/10.1128/AEM.01541-09.
Schubert, M., Lindgreen, S., Orlando, L., 2016. AdapterRemoval v2: rapid adapter trimming, identification, and read merging. BMC Res. Notes 9, 88. https://doi.org/10.1186/s13104-016-1900-2.
Sequino, G., Valentino, V., Esposito, A., Volpe, S., Torrieri, E., De Filippis, F., Ercolini, D., 2024. Microbiome dynamics, antibiotic resistance gene patterns and spoilage-associated genomic potential in fresh anchovies stored in different conditions. Food Res. Int. 175, 113788. https://doi.org/10.1016/j.foodres.2023.113788.
Sequino, G., Valentino, V., Villani, F., De Filippis, F., 2022. Omics-based monitoring of microbial dynamics across the food chain for the improvement of food safety and quality. Food Res. Int. 157, 111242. https://doi.org/10.1016/j.foodres.2022.111242.
Urakawa, H., Kita-Tsukamoto, K., Steven, S.E., Ohwada, K., Colwell, R.R., 1998. A proposal to transfer *Vibrio marinus* (Russell 1891) to a new genus Moritella gen. nov. as *Moritella marina* comb. nov. FEMS (Fed. Eur. Microbiol. Soc.) Microbiol. Lett. 165 (2), 373–378. https://doi.org/10.1111/j.1574-6968.1998.tb13173.x.
Wang, X., Zheng, Z., 2025. Mechanistic insights into fish spoilage and integrated preservation technologies. Appl. Sci. 15 (14), 7639.
Wickham, H., 2016. Programming with ggplot2. In: Wickham, H. (Ed.), ggplot2: Elegant Graphics for Data Analysis. Springer International Publishing, pp. 241–253. https://doi.org/10.1007/978-3-319-24277-4_12.
Wood, D.E., Salzberg, S.L., 2014. Kraken: ultrafast metagenomic sequence classification using exact alignments. Genome Biol. 15 (3), R46. https://doi.org/10.1186/gb-2014-15-3-r46.
Zheng, R., Xu, X., Xing, J., Cheng, H., Zhang, S., Shen, J., Li, H., 2020. Quality evaluation and characterization of specific spoilage organisms of Spanish mackerel by high-throughput sequencing during 0 °C cold chain logistics. Foods 9 (3), 312.